CSIRO PUBLISHING

Publications of the Astronomical Society of Australia, 2010, **27**, 296–301 www.publish.csiro.au/journals/pasa

The Correlated Multi-color Optical Variations of BL Lac Object S5 0716+714

Bingkai Zhang[A,E], *Benzhong Dai*[B], *Li Zhang*[B,C], *Jiali Liu*[D], *and Zhen Cao*[D]

[A] Department of Physics, Fuyang Normal University, Fuyang 236041, China
[B] Department of Physics, Yunnan University, Kunming 650091, China
[C] National Astronomical Observatories/Yunnan Observatory, Chinese Academy of Sciences, P.O. Box 110, Kunming 650011, China
[D] The Key Laboratory of Particle and Astrophysics, Institute of High Energy Physics, Chinese Academy of Sciences, Beijing 100049, China
[E] Corresponding author. Email: zhangbk@mail.ihep.ac.cn

Received 2009 December 1, accepted 2010 March 16

Abstract: S5 0716+714 is a well-studied BL Lac object in the sky. Verifying the existence of correlations among the flux variations in different bands serves as an important tool to investigate the emission processes. To examine the possible existence of a lag between variations in different optical bands on this source, we employ a discrete correlation function analysis on the light curves. In order to obtain statistically meaningful values for the cross-correlation time lags and their related uncertainties, we perform Monte Carlo simulations called 'flux redistribution/random subset selection'. Our analysis confirms that the variations in different optical light curves are strongly correlated. The time lags show a hint of the variations in high frequency band leading those in low frequency band of the order of a few minutes.

Keywords: BL Lacs: general — BL Lacs: individual (S5 0716+714)

1 Introduction

Blazars include BL Lacertae (BL Lac) objects and flat spectrum radio quasars (FSRQs). They are the most extreme class of active galactic nuclei (AGNs) and exhibit strong variability at all wavelengths of the whole electromagnetic (EM) spectrum, strong polarization from radio to optical wavelengths, and are usually core dominated radio structures. These extreme properties are generally interpreted by many authors as a consequence of non-thermal emission from a relativistic jet oriented close to the line of sight (Blandford & Königl 1979; Urry & Padovani 1995). Blazars vary on diverse time scales (Gupta et al. 2008 and references therein). Variability has been one of the most powerful tools in revealing the nature of blazars. Understanding variation behaviour is one of the major issues of AGNs studies. The variability lags between different energy bands provide very important constraints for the interpretation of the emission components. In recent years, correlations of the variability in different energy regions have been widely studied (Raiteri et al. 2001, 2008; Dai et al. 2006; Arévalo et al. 2008; Chatterjee et al. 2008; Marshall et al. 2008; Bonning et al. 2009; Villata et al. 2009).

The radio source S5 0716+714 is one of the brightest and most-studied BL Lacertae objects. It was discovered in 1979 (Kühr et al. 1981), and was classified as a BL Lac object because of its featureless spectrum and its strong optical polarization (Biermann et al. 1981). By optical imaging of the underlying galaxy, its redshift of $z = 0.31 \pm 0.08$ was recently derived (Nilsson et al. 2008). It is a highly variable BL Lac object in the whole EM spectrum on diverse time scales (Heidt & Wagner 1996; Wagner et al. 1996; Ghisellini et al. 1997; Villata et al. 2000; Raiteri et al. 2003; Bach et al. 2005, 2006; Nesci et al. 2005; Pian et al. 2005; Foschini et al. 2006; Montagni et al. 2006; Ostorero et al. 2006; Stalin et al. 2006; Wu et al. 2007). The correlations and time lags between different energy bands in this source have been studied by some authors. A correlation was claimed for a selected range of data at 6 and 3 cm wavelengths, and optical wavelengths by Quirrenbach et al. (1991). But 2 cm data from the same epoch published later by Quirrenbach et al. (2000) does not show evidence for correlated variability, casting doubt on the reliability of the claimed correlation between radio and optical bands (Bignall et al. 2003). A good correlation was noticed between the light curves in the different passbands (Sagar et al. 1999). An upper limit to the possible delay between B and I variations (10 min) was determined by Villata et al. (2000). With the data taken on 1995 January 8, Qian et al. (2000) found an upper limit of the time lag of 0.0041 d between variations in the V and I bands. Raiteri et al. (2003) found that the variations between different radio bands are strongly correlated, and the flux variations at the lower radio frequencies are delayed with respect to those at the higher frequencies. They also found weak correlations between the optical and radio emissions.

 10.1071/AS09086 1323-3580/10/03296

Stalin et al. (2006) analyzed two night data, and found that V and R are correlated with a small time lag (∼6 and 13 min, respectively, for 1996 April 7 and 14) and the variation at V leading that at R on both nights. Chen et al. (2008) studied the gamma-optical correlation. Their result suggested a possible delay in the gamma-ray flux variations with respect to optical (R band) variations of the order of 1 d. Fuhrmann et al. (2008) confirmed the existence of a significant correlation across all their observed radio bands. The time delay between the two most separated bands ($\lambda_{3\,\mathrm{mm}}$ and $\lambda_{60\,\mathrm{mm}}$) is ∼2.5 d. It must be noted that the time delay of 2.5 d is determined from an almost monotonic increase in flux density observed over a time range of 11 d.

The determination of time lag can be used to study the geometry, kinematics, and physical conditions in the inner regions of AGNs. This is attributed to light travel-time effect (Villata et al. 2000). It is very important to search for detectable delays between optical bands themselves, even if these can be expected to be very small, if existent. Our goals in this paper are to investigate the correlations between different optical light curves. The paper is arranged as follows: in Section 2, the light curves are presented; then in Section 3, the correlations and the time lags between different optical passbands are presented; after this, the discussion and conclusions are given in Section 4.

2 Light Curves

S5 0716+714 is a well-monitored object. It has been observed in various multi-frequency campaigns (Wagner et al. 1996; Sagar et al. 1999; Villata et al. 2000, 2008; Stalin et al. 2006). In addition, Ghisellini et al. (1997) presented the results of their optical observations between 1994 November 15 and 1995 April 30. Qian et al. (2002) published *BVRI* band light curves from 1994 to 2000. Raiteri et al. (2003) presented the largest optical database from 1994 to 2001. Xie et al. (2004) also reported their monitoring results on this source. Montagni et al. (2006) introduced a large set of observational data containing 10 675 photometric points. Gu et al. (2006) extensively monitored this source in 2003 and 2004. Zhang et al. (2008) presented the optical photometries (*BVRI*) of the source from 2001 February to 2006 April.

To search for lags between different optical bands, one needs well-sampled and high-quality datasets. Examining the datasets mentioned above, we find the optical photometry presented by Gu et al. (2006) provided a possibility to determine the time lag. The source was observed quasi-simultaneously in four passbands and the overall observations span ∼140 d. Each optical light curve in the *BVRI* bands is well sampled. Furthermore, the source exhibited strong variability during the observations.

The detailed statistics of these data are listed in Table 1. The first column represents the bands, the second represents the numbers, the third represents the mean values, the fourth represents the standard deviations, the fifth represents the largest variations and the last represents the

Table 1. Statistics of *BVRI*-band data of BL Lac object S5 0716+714

Band	N	Mean (mag)	σ (mag)	Δ (mag)	Interval (min)
B	239	14.13	0.38	1.42	11.2
V	287	13.69	0.37	1.37	11.1
R	301	13.28	0.36	1.37	11.1
I	292	12.75	0.35	1.36	11.1

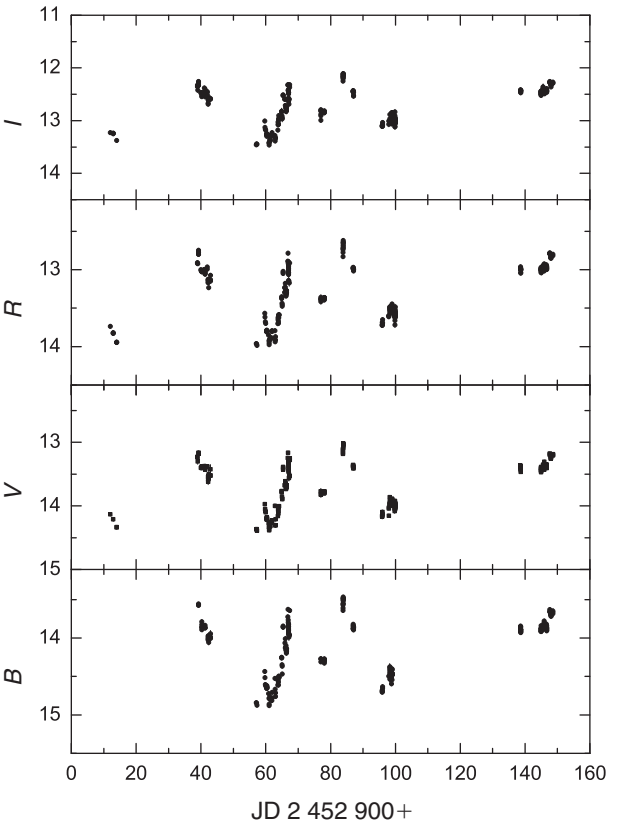

Figure 1 Light curves of S5 0716+714 in the *BVRI* bands.

median interval of the data points. The light curves of different passbands are displayed in Figure 1. They are very similar but different amplitudes. In the light curves, there are some significant substructures. Because of the large time scale, most independent variations cannot be seen. To illustrate the fine structures of variations, Figure 2 shows the light curves during JD 2 452 958–2 452 970. It is clear that the source does not undergo a monotonic increase between JD 2 452 958 and 2 452 970. The data contain many more variations than those indicated by Figure 1. The source exhibits independent variation almost every night.

3 Correlation Analysis

3.1 Discrete Correlation Function Method

The discrete correlation function (DCF) was introduced by Edelson & Krolik (1988). It is a useful method of measuring correlation, and it does not require interpolating in

https://doi.org/10.1071/AS09086 Published online by Cambridge University Press

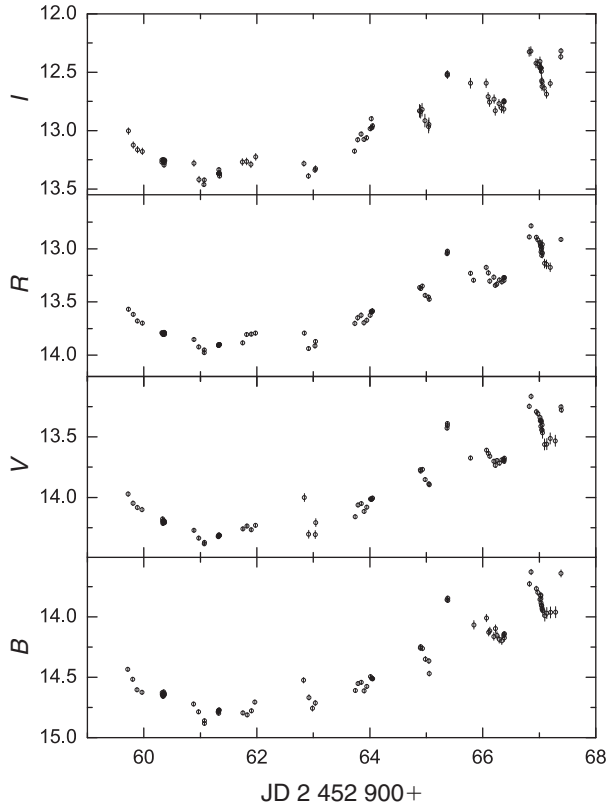

Figure 2 Light curves of S5 0716+714 in the *BVRI* bands during JD 2 452 958–2 452 970.

the temporal domain. This method can not only provide the correlation of two series of unevenly sampled variability data with the time lag, but also give evidence of periodicity that lies in a single temporal dataset. Its other advantages are that it uses all the data points available and calculates a meaningful error estimate. Our first step is to calculate the set of un-binned discrete correlations (UDCF) between each data point in the two data streams. It is defined as follows:

$$UDCF_{ij} = \frac{(a_i - \overline{a}) \times (b_j - \overline{b})}{\sqrt{\sigma_a^2 \times \sigma_b^2}}, \quad (1)$$

where a_i and b_j are points of the datasets a and b, $\overline{a}$ and $\overline{b}$ are the means of the datasets a and b, and σ_a and σ_b are the standard deviations of each dataset. Each UDCF is associated with the pair-wise lag $\Delta t_{ij} = t_j - t_i$. Then we average over the M pairs for which $\tau - \Delta\tau/2 \leq \Delta t_{ij} < \tau + \Delta\tau/2$, and obtain the DCF:

$$DCF(\tau) = \frac{1}{M} \sum UDCF_{ij}(\tau), \quad (2)$$

where M is the number of pairs in the bin. When $a = b$, the autocorrelation DCF is produced, and when $a \neq b$, the cross-correlation DCF is measured. In most cases, the evident peak in the cross-correlation function means a strong correlation between two data series, and the peak in the autocorrelation DCF implies a strong period in the dataset.

The standard error for each bin is defined as

$$\sigma(\tau) = \frac{1}{M-1} \left\{ \sum [UDCF_{ij} - DCF(\tau)]^2 \right\}^{1/2}. \quad (3)$$

In order to obtain statistically meaningful values for the cross-correlation time lags and their related uncertainties, it is common usage to calculate the centroid τ_c of the DCF, given by

$$\tau_c = \frac{\sum_i \tau_i DCF_i}{\sum_i DCF_i}, \quad (4)$$

where sums run over the points which have a DCF value close to the peak value ($DCF_i > 0.8 DCF_{\rm peak}$), then perform Monte Carlo simulations known as 'flux redistribution/random subset selection' (FR/RSS) described in detail by Peterson et al. (1998) and Raiteri et al. (2003). Random subsets of the two datasets to be correlated are selected, redundant points are discarded, and random gaussian deviates constrained by the flux errors are added to the fluxes; thus, the influence of both uneven sampling and flux density errors is taken into account. In each simulation, the two subsets are then cross-correlated and the centroid τ_c of the DCF peak is determined. After a large number of simulations (generally 500∼2000), the cross-correlation peak (actually, the centroid) distribution (CCPD) is obtained. As measures of the time lag and its uncertainties, $\tau_{\rm median}$ and $\pm\Delta\tau_{68}$ can be computed directly from the CCPD, where $\pm\Delta\tau_{68}$ corresponds to 1σ errors for a normal distribution (Peterson et al. 1998).

3.2 Results

According to the above method, we calculate the discrete correlation function (DCF) between different optical bands to search for correlations and possible time lags. Between the *B* and *I* band light curves, the median interval time is 6.3 min. The DCF result computed with a bin size of 10 min is shown in the top left panel of Figure 3. The curve of DCF has an obvious maximum at the position of 10 min. The maximum value of DCF is 1.1 ± 0.1. The centroid τ_c corresponding to this peak is 0.1 min. To give a statistically reliable result, we perform Monte Carlo simulations. Because the possible delay is of the same magnitude as the DCF bin size and of the light curve time resolution, the effect of bin size cannot be ignored. To eliminate the effect caused by the choice of the bin size, we calculate the DCF with different bin sizes, from 8 to 15 min. The lack of better sampling does not allow us to improve the bin size resolution without increasing spurious effects too much. We perform 1000 Monte Carlo simulations for each bin size, thus 8000 Monte Carlo simulations are performed. The CCPD is obtained and plotted in the top right panel of Figure 3. From this, the time lag and the uncertainties of $10.2^{-20.7}_{+13.8}$ min are derived. In addition, the mean $DCF_{\rm peak}$ of 1.2 ± 0.1 is achieved by 8000 Monte simulations. This means that the variation of *B* band is strongly correlated with that of *I* band with leading about $10.2^{-20.7}_{+13.8}$ min.

This procedure is applied to each two bands of *BVRI*. The DCFs and CCPDs are plotted in Figures 3 and 4.

https://doi.org/10.1071/AS09086 Published online by Cambridge University Press

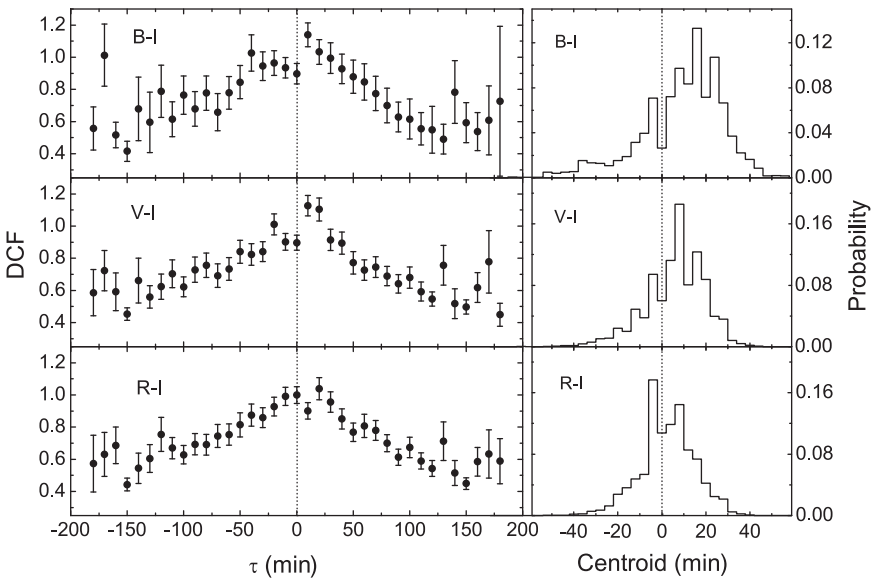

Figure 3 Left: DCFs between B and I, V and I, R and I, respectively. Right: Normalized CCPDs relative to the central peak obtained by running 8000 FR/RSS Monte Carlo simulations. Dashed vertical lines are drawn to guide the eye.

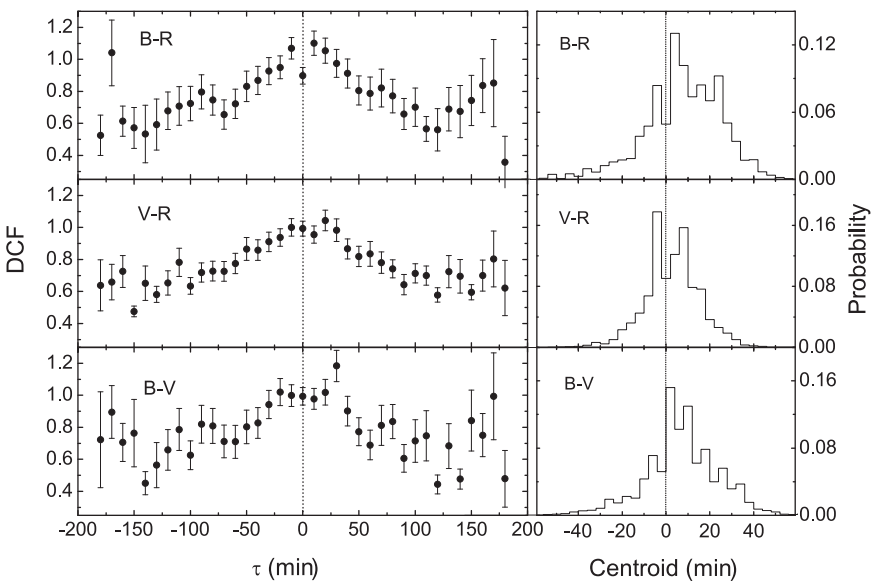

Figure 4 Left: DCFs between B and R, V and R, B and V, respectively. Right: Normalized CCPDs relative to the central peak obtained by running 8000 FR/RSS Monte Carlo simulations. Dashed vertical lines are drawn to guide the eye.

The results are shown in Table 2. The first column gives the band, the second gives the median time interval of two bands, the third gives the possible delay, and the last gives the mean value of $DCF_{\rm peak}$s. The results suggest the existence of significant correlation among $BVRI$ band light curves and that the higher frequencies vary earlier.

4 Discussion and Conclusions

It is well known that the light curves between variant wave bands may have a short time lag. According to the inhomogeneous jet models, time delays are expected

Table 2. The possible time lags determined by DCF

Band	Interval (min)	Lag (min)	$DCF_{\rm peak}$
$B-I$	6.3	$10.2^{-20.7}_{+13.8}$	1.2 ± 0.1
$V-I$	4.9	$5.8^{-14.9}_{+11.4}$	1.1 ± 0.1
$R-I$	3.7	$0.2^{-11.3}_{+12.4}$	1.0 ± 0.1
$B-R$	5.3	$6.0^{-15.9}_{+16.9}$	1.1 ± 0.1
$V-R$	4.3	$0.3^{-10.6}_{+12.3}$	1.1 ± 0.1
$B-V$	5.2	$5.6^{-14.6}_{+16.8}$	1.1 ± 0.1

https://doi.org/10.1071/AS09086 Published online by Cambridge University Press

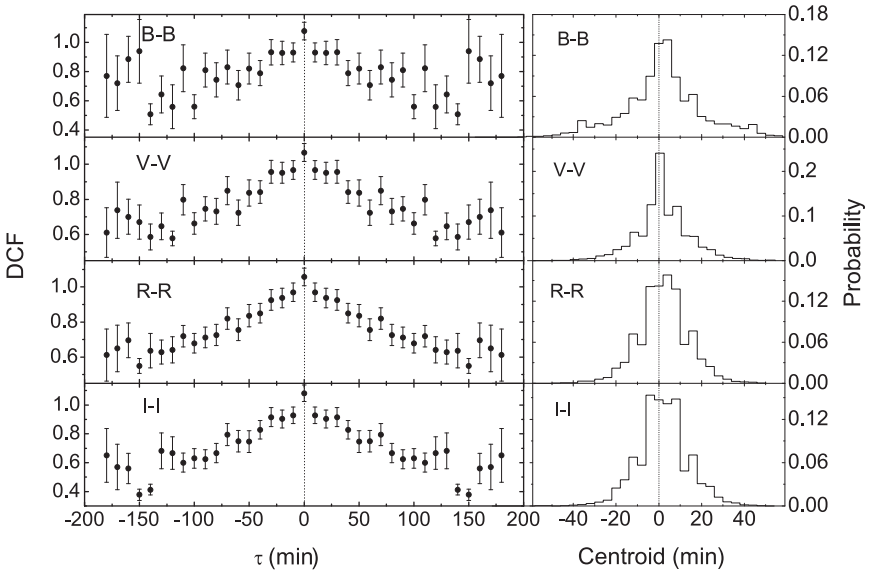

Figure 5 Left: Auto-DCFs of $B-B$, $V-V$, $R-R$, and $I-I$, respectively. Right: Normalized CCPDs relative to the central peak obtained by running 8000 FR/RSS Monte Carlo simulations. Dashed vertical lines are drawn to guide the eye.

Table 3. Test results between light curves and their corresponding shifted light curves[a]

t	lag_B	lag_V	lag_R	lag_I
1	$0.4^{-13.9}_{+14.4}$	$0.7^{-11.5}_{+12.0}$	$0.6^{-11.7}_{+12.3}$	$0.5^{-11.4}_{+12.9}$
2	$3.0^{-13.3}_{+12.0}$	$1.0^{-9.9}_{+11.4}$	$0.9^{-11.2}_{+12.5}$	$0.6^{-11.4}_{+13.2}$
3	$1.3^{-12.0}_{+14.9}$	$3.9^{-11.1}_{+9.9}$	$4.0^{-12.3}_{+10.1}$	$3.4^{-11.7}_{+11.2}$
4	$4.5^{-15.2}_{+15.0}$	$4.7^{-11.1}_{+11.4}$	$4.9^{-11.1}_{+11.6}$	$4.6^{-10.9}_{+12.0}$
5	$4.6^{-15.3}_{+14.3}$	$4.6^{-10.9}_{+10.8}$	$4.9^{-11.3}_{+11.6}$	$4.9^{-11.6}_{+10.6}$
6	$5.7^{-12.8}_{+12.4}$	$5.7^{-10.8}_{+10.0}$	$5.8^{-11.8}_{+11.8}$	$5.8^{-11.9}_{+11.2}$
7	$7.1^{-14.8}_{+14.4}$	$7.0^{-11.7}_{+12.6}$	$7.3^{-12.7}_{+12.9}$	$6.9^{-12.2}_{+12.9}$
8	$8.0^{-15.5}_{+16.6}$	$8.4^{-12.2}_{+12.4}$	$8.4^{-12.7}_{+12.4}$	$7.8^{-12.3}_{+13.3}$
9	$9.3^{-12.3}_{+14.6}$	$9.5^{-10.0}_{+11.1}$	$9.2^{-9.7}_{+12.4}$	$8.8^{-11.7}_{+12.5}$
10	$10.6^{-15.7}_{+12.6}$	$10.2^{-10.1}_{+10.4}$	$10.3^{-10.2}_{+11.5}$	$10.0^{-9.9}_{+12.0}$

[a]The mean of each column can be seen in the text, and all the above are in units of minutes.

between the emission in different energy bands as plasma disturbances propagate downstream (Georganopoulos & Marscher 1998). Multi-wavelength monitoring of blazars shows that flares usually begin at high frequencies and then propagate to lower frequencies, implying that high-frequency synchrotron emission arises closer to the core than low-frequency synchrotron emission (Ulrich et al. 1997; Marscher 2001). High-energy electrons emit synchrotron radiation at high frequencies and then cool, emitting at progressively lower frequencies and resulting in time lags between high and low frequencies (Bai & Lee 2005). The small time lags in optical regimes may be result of very small frequency intervals, and may indicate that the photons in these wavelengths should be produced by the same physical process.

The above results have been obtained with a light-curve time resolution of the same magnitude as the possible lag. To check the method and the result mentioned above, we calculate the $B-B$ band autocorrelation DCF (Figure 5). The result of Monte Carlo simulations suggests that the time delay is $-0.0^{-16.3}_{+15.5}$ min. For the $V-V$, $R-R$, and $I-I$ autocorrelations, τ is $0.0^{-11.4}_{+11.6}$, $0.1^{-11.5}_{+12.0}$, and $-0.0^{-11.5}_{+11.8}$ min, respectively (see Figure 5). They are all consistent with the expectation of zero lags. Furthermore, we shift $BVRI$ band light curves by a time $t_{\rm shift}$ and generate the corresponding artificial light curves of $B_{\rm shift}$, $V_{\rm shift}$, $R_{\rm shift}$, and $I_{\rm shift}$. Using the same process, we search for the time lag between the light curve and the shifted light curve. The results are listed in Table 3. The first column is the shifted time, the second to the last are for the lags of $B-B_{\rm shift}$, $V-V_{\rm shift}$, $R-R_{\rm shift}$, and $I-I_{\rm shift}$ determined by the method introduced above. From the results listed in Table 3, one can see that the lags between two correlated light curves can be well determined. In addition to shifting the light curves to calculate the displaced auto-DCF peaks, we shift the light curves with respect to those at each other wavelength by the time lags determined. The resulting DCFs are more consistent with zero lag. So, the time lags between different optical $BVRI$ band light curves are more reliable.

The time lag of 10.2 min between variations of B and I band is consistent with the result found by Villata et al. (2000). They derived an upper limit of 10 min between B and I variations. The 5.8-min lag between the band V and I is in good agreement with the 0.0041-d lag determined by Qian et al. (2000). For the V and I band variations, Stalin et al. (2006) reported time lags of ∼6 and 13 min on two individual nights. Between the V' and R' band variations, Wu et al. (2007) obtained the lags of 2.34 ± 5.25 min on JD 2 453 737 and -0.01 ± 1.88 min on JD 2 453 742. Because the time lags are very short, shorter than their typical sampling interval, they concluded that they did not detect an apparent time lag. In this analysis, it also must be pointed

https://doi.org/10.1071/AS09086 Published online by Cambridge University Press

out that the time lags between the different optical bands are of the same orders of the light-curve time resolution, and the uncertainties are larger than the lags. So, the lags should be treated with caution, and much more significant results can only be achieved with much denser monitoring data. Two ways were suggested by Villata et al. (2000) to improve the time resolution of the light curves: one way is to enlarge the telescope, another is the synchronized use of two or more telescopes.

In summary, the variations between different optical bands have been analyzed and the time lags and their uncertainties are convincingly determined. The results suggest that the variations are very strongly correlated. Considering the errors, each one of the values agrees well with zero lag. While looking at the whole set of lags, it is possible to say that there is a hint of the variations of high frequency bands leading those of low frequency bands in the order of a few minutes.

Acknowledgments

We express our thanks to the people who helped with this work, and acknowledge the valuable suggestions from the peer reviewers. This work is supported by the Research Foundation of Education Department of Anhui Province, China (KJ2010B159), National Natural Science Foundation of China (10975145) and Fuyang Normal University, also partly by Natural Science Foundation of Yunnan Province (2007A026M) and the Innovation fund (U-526) of the Institute of High Energy Physics.

References

Arévalo, P. et al., 2008, MNRAS, 389, 1479
Bach, U. et al., 2005, A&A, 433, 815
Bach, U. et al., 2006, A&A, 452, 83
Bai, J. M. & Lee, M. G., 2003, ApJ, 585, L113
Biermann, P. et al., 1981, ApJ, 247, L53
Bignall, H. E. et al., 2003, ApJ, 585, 653
Blandford, R. D. & Königl, A., 1979, ApJ, 232, 34
Bonning, E. W. et al., 2009, ApJ, 697, L81
Chatterjee, R. et al., 2008, ApJ, 689, 79
Chen, A. W. et al., 2008, A&A, 489, L37
Dai, B. Z., Zhang, B. K. & Zhang, L., 2006, NewA, 11, 471
Edelson, R. A. & Krolik, J. H., 1988, ApJ, 333, 646
Foschini, L. et al., 2006, A&A, 455, 871
Fuhrmann, L. et al., 2008, A&A, 490, 1019
Georganopoulos, M. & Marscher, A. P., 1998, ApJ, 506, L11
Ghisellini, G. et al., 1997, A&A, 327, 61
Gu, M. F. et al., 2006, A&A, 450, 39
Gupta, A. C., Fan, J. H., Bai, J. M. & Wagner, S. J., 2008, AJ, 135, 1384
Heidt, J. & Wagner, S. J., 1996, A&A, 305, 42
Kühr, H. et al., 1981, AJ, 86, 854
Marscher, A. P., 2001, ASPC, 224, 23
Marshall, K., Ryle, W. T. & Miller, H. R., 2008, ApJ, 677, 880
Montagni, F. et al., 2006, A&A, 451, 435
Nesci, R. et al., 2005, AJ, 130, 1466
Nilsson, K., Pursimo, T., Sillanpää, A., Takalo, L. O. & Lindfors, E., 2008, A&A, 487, L29
Ostorero, L. et al., 2006, A&A, 451, 797
Peterson, B. M. et al., 1998, PASP, 110, 660
Pian, E. et al., 2005, A&A, 429, 427
Qian, B., Tao, J. & Fan, J., 2000, PASJ, 52, 1075
Qian, B., Tao, J. & Fan, J., 2002, AJ, 123, 678
Quirrenbach, A. et al., 1991, ApJ, 372, L71
Quirrenbach, A. et al., 2000, A&AS, 141, 221
Raiteri, C. M. et al., 2001, A&A, 377, 396
Raiteri, C. M. et al., 2003, A&A, 402, 151
Raiteri, C. M. et al., 2008, A&A, 480, 339
Sagar, R., Gopal-Krishna, M. V., Pandey, A. K., Bhatt, B. C. & Wagner, S. J., 1999, A&AS, 134, 453
Stalin, C. S. et al., 2006, MNRAS, 366, 1337
Ulrich, M. H., Maraschi, L. & Urry, C. M., 1997, ARA&A, 35, 445
Urry, C. M. & Padovani, P., 1995, PASP, 107, 803
Villata, M. et al., 2000, A&A, 363, 108
Villata, M. et al., 2008, A&A, 481, L79
Villata, M. et al., 2009, A&A, 501, 455
Wagner, S. J. et al., 1996, AJ, 111, 2187
Wu, J. et al., 2005, AJ, 129, 1818
Wu, J. et al., 2007, AJ, 133, 1599
Xie, G. Z. et al., 2004, MNRAS, 348, 831
Zhang, X. et al., 2008, AJ, 136, 1846